Materials Science and Engineering B 176 (2011) 442–445

Contents lists available at ScienceDirect

Materials Science and Engineering B

journal homepage: www.elsevier.com/locate/mseb

Short communication

Ag–Sb composite prepared by chemical reduction method as new anode materials for lithium-ion batteries

Fei Wang[a], Gang Yao[a], Minwei Xu[a], Mingshu Zhao[a,*], Peixin Zhang[b], Xiaoping Song[a,**]

[a] MOE Key Laboratory for Nonequilibrium Synthesis and Modulation of Condensed Matter, School of Science, Xi'an Jiaotong University, Xi'an 710049, PR China
[b] School of Chemistry and Chemical Engineering, Shenzhen University, 518060, PR China

ARTICLE INFO

Article history:
Received 29 June 2010
Received in revised form
27 September 2010
Accepted 30 October 2010

Keywords:
Lithium-ion battery
Anode
Ag–Sb composite
Cycling performance

ABSTRACT

Ag–Sb composite anode was prepared by chemical reductive method. The structure, morphology, chemical composition and electrochemical properties of synthesized Ag–Sb composite anode were evaluated by XRD, FE-SEM, EDS and galvanostatical charge–discharge tests. The results indicated that the changes of structure and volume were alleviated effectively by using metal phase instead of intermetallic phase and restraining the lithiation reaction of Ag at high current density (0.2 mA cm^{-2}). The electrochemical reactions took place in a stable and highly conductive Ag framework, which ensured the good cyclability of the Ag–Sb composite electrode.

1. Introduction

Lithium-ion batteries have been considered as attractive power sources for using in various electronic devices due to their superior performance compared to other available batteries. Graphite is widely used as negative electrode in commercial lithium-ion batteries. However, the low theoretical capacity and safety problem of graphite cannot meet the increasing demands of higher performance batteries, which urges researchers to explore novel alternative negative materials. Most active metals, such as Sn, Sb, Si, Al, etc., are generally regarded as possible negative materials for lithium-ion batteries. They can offer much higher energy density and specific capacity than those of the carbonaceous materials. Nevertheless, these metals undergo severe volumetric changes during lithiation/delithiation processes, which greatly limits the cycle life of the electrodes [1–3]. Decreasing particle size of metals to nano-scale is an effective way to alleviate the impact of volumetric changes and thus enhance the mechanical stability [2,3]. Meanwhile, the big specific surface area and short Li^+ diffusion path in nano-scale materials are also beneficial for electrode kinetics. However, the electrochemical aggregation tends to appear when the particle size of active metal/alloy materials is too small [4,5]. Another method to improve the cycling performance of active metals can be used by utilizing a 'buffer matrix' to compensate for the expansion of reactants and thus preserve the conductive pathway [6,7], such as tin oxides [8–10], amorphous tin composite oxides (ATCO) [11] and intermetallic compounds [12–16]. The application of tin oxides and ATCO is limited owing to their inherent high initial irreversible capacities. For intermetallic compounds, the complicated structural changes as well as volumetric changes during lithiation/delithiation processes reduce the reversibility of electrode materials. Therefore, using binary metal composites instead of intermetallic compounds should be an effective strategy to alleviate the impact of structural changes. Furthermore, the electrochemical aggregation of nano-scale active component should be alleviated if the active component is dispersed uniformly in more stable inactive one.

In this paper, we used chemical reductive method, a facile and controllable method for large-scale synthesis of metals, intermetallic compounds and composites, to prepare nano-scale Ag–Sb composite with metal phases instead of intermetallic compound phase. The electrochemical performances of it were also investigated by galvanostatical charge–discharge tests as anode materials for lithium ion batteries.

2. Experimental

The Ag–Sb composite powders were synthesized by reductive precipitation method from $AgNO_3$ and $SbCl_3$ aqueous solutions with $NaBH_4$. At first, 0.3397 g $AgNO_3$ aqueous solution (0.1 M) was added drop-wise to 0.3416 g alkaline $NaBH_4$ aqueous solution (0.2 M, pH > 12) under strong magnetic stirring at room temperature. And then, the mixed aqueous solution of 0.4562 g $SbCl_3$ (0.1 M) and 1.7646 g $C_6H_5Na_3O_7{\cdot}2H_2O$ was added drop-wise to

* Corresponding author. Tel.: +86 29 82663034; fax: +86 29 82667872.
** Corresponding author. Tel.: +86 29 82665892; fax: +86 29 82667872.
E-mail addresses: zhaomshu@mail.xjtu.edu.cn (M. Zhao), xpsong@mail.xjtu.edu.cn (X. Song).

0921-5107/$ – see front matter © 2010 Elsevier B.V. All rights reserved.
doi:10.1016/j.mseb.2010.10.019

the above $NaBH_4$ aqueous solution subsequently. The superfluous $NaBH_4$ was used to ensure the complete reduction of the metal ions in the solution. The precipitates in aqueous solution were aged in the water bath with a constant temperature of 80 °C for 5 h. Afterwards, the suspension was filtered and the product was washed thoroughly by distilled water and acetone. The obtained black product was dried at 105 °C for 10 h under vacuum. The antimony and silver powders were synthesized by similar method mentioned above, respectively.

The crystal structure of the Ag–Sb composite was detected by Shimadzu-7000 X-ray diffractometer (XRD) with Cu Kα radiation. The morphology of the Sb, Ag and Ag–Sb composite was characterized by JSM-6700 field-emission scanning electron microscope (FE-SEM). The chemical composition of Ag–Sb composite were analyzed by energy disperse spectroscopy (EDS) in above FE-SEM.

Electrochemical experiments were carried out in two-electrode Swagelok cell, which was composed by a metallic lithium foil as the counter electrode, 1 M $LiPF_6$ in ethylene carbonate (EC)–diethyl carbonate (DEC) (1:1, v/v) as the electrolyte, Celegard 2400 as the separator and obtained products as the working electrode. The working electrodes were prepared by coating the slurry of Sb or Ag–Sb composite onto a copper foil substrate. The slurry consisted of 80 wt% Sb or Ag–Sb composite, 10 wt% acetylene black and 10 wt% polyvinylidene fluoride (PVDF) dissolved in 1-methyl-2-pyrrolydon (NMP). The working electrodes were dried under vacuum at 110 °C for 12 h before use. The testing cells were assembled in an argon-filled glove box and tested by galvanostatical charge–discharge mode on the Arbin BT2000 battery tester at various current densities between 0.02 and 1.5 V.

3. Results and discussion

The X-ray diffraction pattern of the Ag–Sb composite and standard XRD patterns of Ag, Sb and Ag_3Sb taken from the JCPDS database are shown in Fig. 1. From it we can see clearly that the

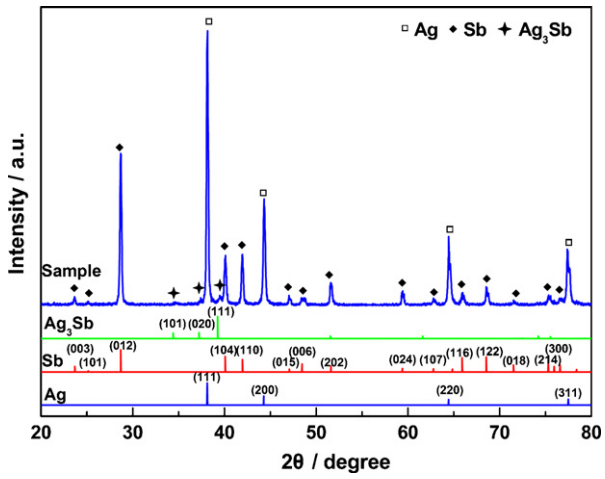

Fig. 1. XRD pattern of Ag–Sb composite powders prepared by reductive precipitation method.

diffraction pattern of Ag–Sb composite contains sharp Ag, Sb peaks and weak Ag_3Sb peaks, which indicate that only little amount of Ag_3Sb intermetallic compound formed by this method. The formation of metal phase instead of intermetallic phase is attributed that the reduction of $AgNO_3$ is finished before $SbCl_3$ was added. The early formed silver becomes stable soon due to the fast nucleation and growth processes, which restrain Ag to form Ag_3Sb intermetallic compound with late formed antimony.

Fig. 2a–c shows the FE-SEM images of the Sb, Ag and Ag–Sb composite obtained by reductive precipitation method. From Fig. 2a and b we can see that both Sb and Ag have narrow size distributing and the particle size of Sb is much smaller than Ag. When $SbCl_3$ and $AgNO_3$ were reduced in same solution, the Ag–Sb composite with smaller Sb particles well dispersed in larger Ag particles was

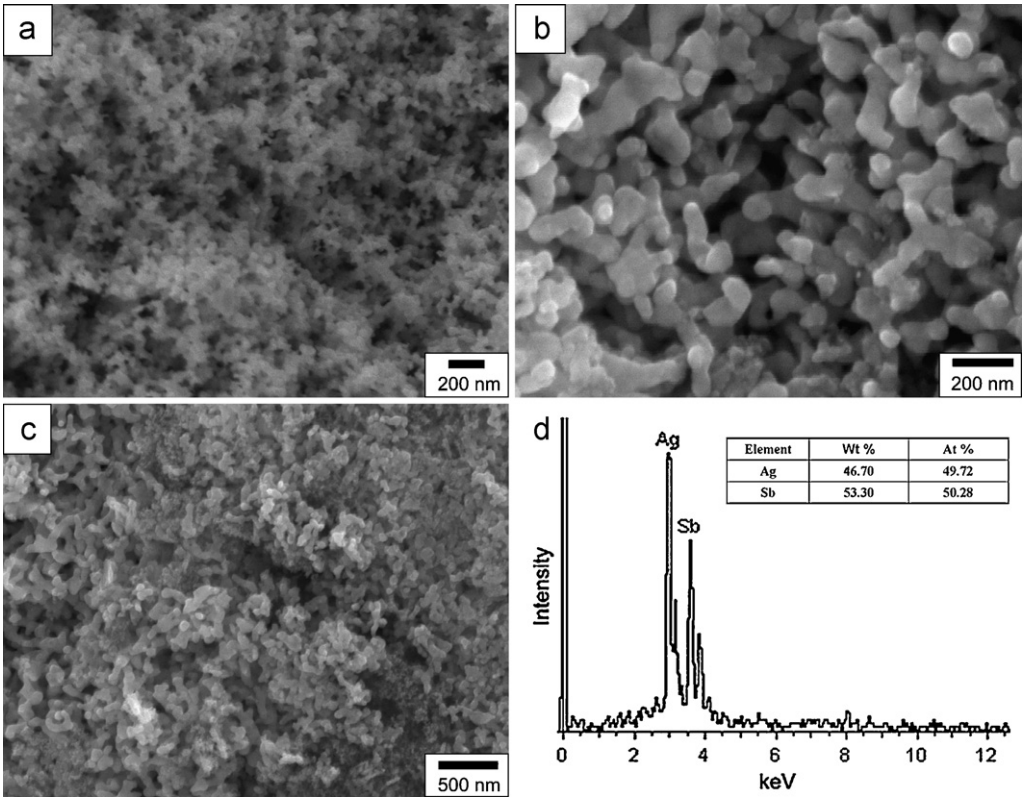

Fig. 2. FE-SEM images of Sb (a), Ag (b) and Ag–Sb composite (c); EDS spectrum of Ag–Sb composite (d).

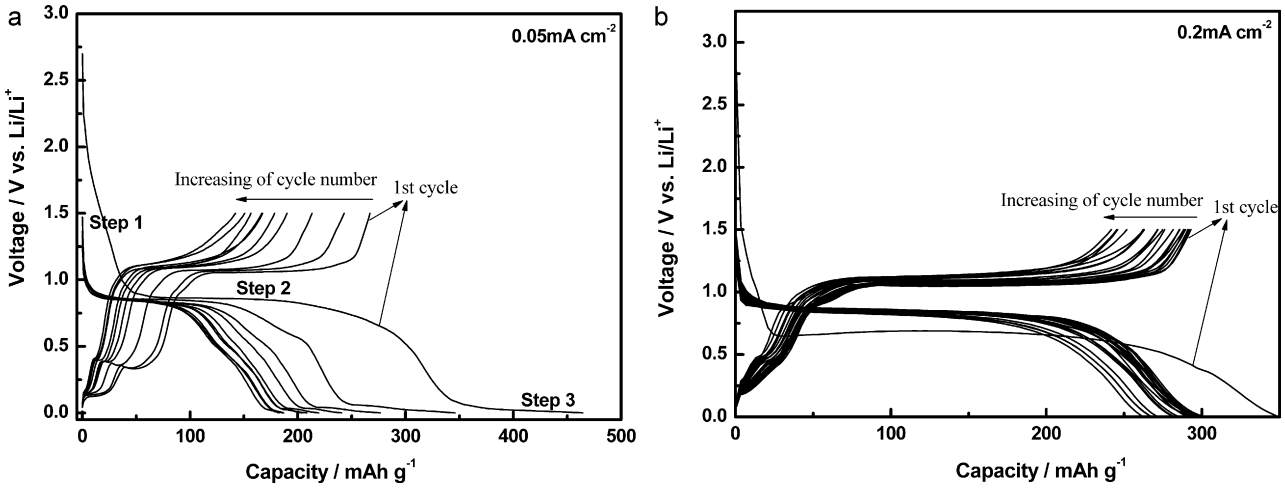

Fig. 3. Voltage profiles of Ag–Sb composite tested at different current densities: (a) 0.05 mA cm^{-2}; (b) 0.2 mA cm^{-2}.

obtained, as shown in Fig. 2c. EDS spectrum shows that the atom ratio of Sb to Ag is about 1:1, which accords with the mol ratio of the precursors.

The voltage versus specific capacity curves of the Ag–Sb composite at different current densities are shown in Fig. 3. The discharge curve of the first cycle can be divided into three steps, which correspond to the various reaction processes. The voltage slope above 0.8 V is attributed to some irreversible reactions, such as electrolyte decomposition, the formation of solid electrolyte interphase (SEI) film and the reduction of oxide impurity. And then, a voltage plateau at about 0.8 V appears, which corresponds to the lithiation reaction of Sb to form Li_3Sb phase. In the third step, a voltage plateau below 0.1 V, lithium further reacts with Ag to form Li_xAg ($1 < x < 4$) phase [17].

From Fig. 3 we can see that the lithiation process is affected obviously by the charge–discharge current densities, especially in the third part. When the Ag–Sb composite is tested at low current density (0.05 mA cm^{-2}), the plateau below 0.1 V is clearly seen in the discharge curve, as shown in Fig. 3a. The lithiation reaction of Ag is restrained and thus the voltage plateau below 0.1 V disappears completely when the Ag–Sb composite is tested at high current density (0.2 mA cm^{-2}), as shown in Fig. 3b. The distinguishing discharge curves tested at different current density are caused by the impact of voltage hysteresis, which result in the moving of actual voltage curves to low-voltage direction in discharge process. And the higher current density is used, the more serious voltage hysteresis appears. Therefore, the actual lithiation reaction voltage of Ag is lower than 0.02 V, the low cut-off voltage in testing, at the current density of 0.2 mA cm^{-2}. On the contrary, reducing reaction rate can alleviate the impact of voltage hysteresis and make the reaction process close to near-equilibrium conditions [18]. Therefore, silver can partly react with Li above 0.02 V at the current density of 0.05 mA cm^{-2}.

The cyclabilities of the Ag–Sb composite at different current densities are shown in Figs. 3 and 4. When the electrode is tested at 0.05 mA cm^{-2}, it has the highest initial capacity due to the additional reaction of Li with Ag at low current density. Whereas, both steps 2 and 3 have fast capacities fade in this case. The more severe volumetric changes appear when Ag takes part in the lithiation reaction, which destroy the stabilization of the surrounding Ag matrix and lead to the losing of electrical contact among particle or between particles and current collector. On the contrary, when the reaction of Li with Ag is restrained by increasing the current density to 0.2 mA cm^{-2}, silver exists just as a matrix in the Ag–Sb composite. The capacities fade caused by the volumetric and structural changes of 'inactive' Ag is alleviated effectively in this case. The electrochemical reactions take place in a stable and highly conductive Ag framework, which ensures the good cyclability and rate performance. Then a considerable improvement of cycling performance is obtained with an electrode capacity above 260 mAh g^{-1} after 22 cycles, which is 74% of the AgSb theoretical capacity when Ag is regarded as 'inactive' element. For comparison, we also provide the cycling performance of Sb (as shown in Fig. 2a) in the inset of Fig. 4. From it we can see that the cyclability of Sb is improved obviously when Ag 'buffer matrix' is used.

From Fig. 3 we can also note that the coulomb efficiency of the Ag–Sb composite electrode cycled at 0.2 mA cm^{-2} exceeds 86% in the first cycle. The high initial coulomb efficiency is attributed to the stability and relatively large particle size of the Ag particles, which lead to very limited irreversible reactions. We know that many strategies to improve the cyclability of active metal anodes may result in high initial irreversible capacity [19], which greatly limits their practical application. So the synthesized Ag–Sb composite electrode in this study is a novel attempt to improve the cyclability of active metal anodes.

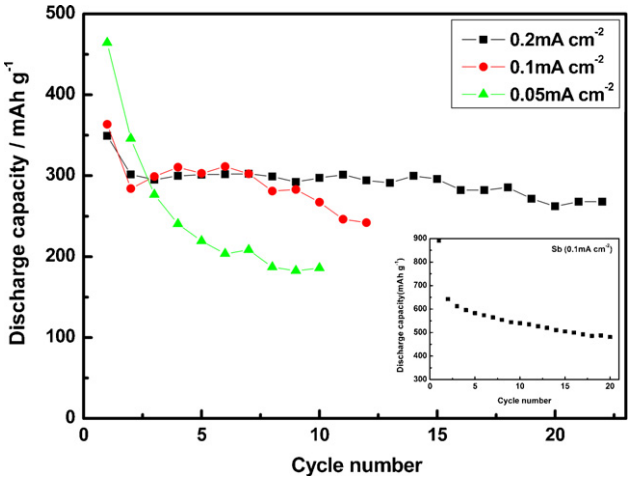

Fig. 4. Cycling performances of Ag–Sb composite tested at different current densities and Sb tested at 0.1 mA cm^{-2} (inset).

4. Conclusions

In this work we have investigated the Ag–Sb composite anode prepared by chemical reductive method. When we used metal phases instead of an intermetallic phase and restrained the lithiation reaction of Ag at high current density ($0.2\,mA\,cm^{-2}$), the structure and volumetric changes were alleviated effectively. The lithiation/dilithiation reactions of Sb took place in a stable and highly conductive Ag framework, which ensured the good cyclability of the Ag–Sb composite electrode.

Acknowledgements

This work was supported by the National Basic Research Program of China (No. 2010CB635101), National Natural Science Foundation of China (51002117) and Support Program for New Teacher in XJTU (0109-08141012).

References

[1] J. Yang, M. Winter, J.O. Besenhard, Solid State Ionics 90 (1–4) (1996) 281–287.
[2] H. Li, X.J. Huang, L.Q. Chen, Z.G. Wu, Y. Liang, Electrochem. Solid State Lett. 2 (11) (1999) 547–549.
[3] M. Winter, J.O. Besenhard, Electrochim. Acta 45 (1–2) (1999) 31–50.
[4] H. Li, X.J. Huang, L.Q. Chen, G.W. Zhou, Z. Zhang, D.P. Yu, Y.J. Mo, N. Pei, Solid State Ionics 135 (1–4) (2000) 181–191.
[5] H. Li, L.H. Shi, W. Lu, X.J. Huang, L.Q. Chen, J. Electrochem. Soc. 148 (8) (2001) A915–A922.
[6] J.M. Tarascon, M. Armand, Nature 414 (6861) (2001) 359–367.
[7] A. Anani, S. Crouchbaker, R.A. Huggins, J. Electrochem. Soc. 134 (12) (1987) 3098–3102.
[8] Z. Ying, Q. Wan, H. Cao, Z.T. Song, S.L. Feng, Appl. Phys. Lett. 87 (11) (2005) 113108.
[9] Y. Wang, H.C. Zeng, J.Y. Lee, Adv. Mater. 18 (5) (2006) 645–649.
[10] S.J. Han, B.C. Jang, T. Kim, S.M. Oh, T. Hyeon, Adv. Funct. Mater. 15 (11) (2005) 1845–1850.
[11] Y. Idota, T. Kubota, A. Matsufuji, Y. Maekawa, T. Miyasaka, Science 276 (5317) (1997) 1395–1397.
[12] F. Wang, M.S. Zhao, X.P. Song, J. Power Sources 175 (1) (2008) 558–563.
[13] M.M. Thackeray, J.T. Vaughey, A.J. Kahaian, K.D. Kepler, R. Benedek, Electrochem. Commun. 1 (3–4) (1999) 111–115.
[14] J.T. Vaughey, J. O'Hara, M.M. Thackeray, Electrochem. Solid State Lett. 3 (1) (2000) 13–16.
[15] L.M.L. Fransson, J.T. Vaughey, R. Benedek, K. Edstrom, J.O. Thomas, M.M. Thackeray, Electrochem. Commun. 3 (7) (2001) 317.
[16] M.M. Thackeray, J.T. Vaughey, C.S. Johnson, A.J. Kropf, R. Benedek, L.M.L. Fransson, K. Edstrom, J. Power Sources 113 (1) (2003) 124–130.
[17] J.T. Vaughey, L. Fransson, H.A. Swinger, K. Edstrom, M.M. Thackeray, J. Power Sources 119 (2003) 64–68.
[18] G. Taillades, J. Sarradin, J. Power Sources 125 (2) (2004) 199–205.
[19] J.G. Ren, X.M. He, W.H. Pu, C.Y. Jiang, C.R. Wan, Electrochim. Acta 52 (4) (2006) 1538–1541.